Light Exoskeleton Design With Topology Optimisation and FEM Simulations for FFF Technology

Submitted: 15th June 2021; accepted: 14th September 2021

Piotr Falkowski

DOI: 10.14313/JAMRIS/2-2021/9

Abstract:
Among past years interest in robot-assisted rehabilitation arose significantly; thus, constructions such as exoskeletons are involved in this process much more often. As patient's bio-signals may be included in a control loop of these devices, they may be also used to support the motion of extremities in an everyday life. Therefore, a field of control over them stays a popular research topic. For this reason, an exoskeleton described in a paper was designed. The most important aim of a project was to enable all anatomical movements within ranges required for the lifting of an object while minimising a mass of the device. The following paper consist of a concept of an exoskeleton and description of FEM simulations and topology optimisation applied to decrease the amount of material needed. Moreover, as an exoskeleton was built with FFF 3-D printing technology, created parts are modelled orthotopically based on nominal mechanical parameters of filaments and directions of their beams. The design is complemented with a short description of control with EMG signals and analysis of load on a user's musculoskeletal system.

Keywords: *exoskeleton, rapid prototyping, rehabilitation robotics, topology optimisation*

1. Introduction

Dynamic development of technology contributed to the creation of new fields of study. Many of them are just combinations of conventional ones. Among others, medical and rehabilitation robotics became especially prospective, due to current high interest in health [5].

A significant focus of rehabilitation robotics is dedicated to exoskeletons [5]. These devices may be either used for physical therapy, supporting everyday mobility of a user or to affect other systems. They may be controlled mechanically or by tracking biosignals with methods such as EMG or EEG [11].

As different approaches may be used to control robots with biosignals, they are still an important topic to research on. A presented project of an exoskeleton is designed to test possibilities of different EMG-based methods, including direct control over motors.

As the whole system supposed to be carried by a user, its mass has to be minimised. Therefore, innovative methods such as topology optimisation and FEM (finite elements method) analysis are involved. Moreover, at the early stage, an exoskeleton is being modified within a lean cycle. Thus, it needs to be buildable rapidly and not to generate high costs of production. For these reasons, 3D printing is considered as the most effective technology. However, combining 3D printing with computer strength analysis is not commonly applicable due to orthotropic material properties based on a printout geometry. This paper presents an approach towards this problem presented for the real case.

2. Concept of a Device

A designed exoskeleton (see figure 1) of two driven degrees of freedom (2 DOFs) supposed to support lifting by an upper extremity of a human. It shall be usable by people suffering from musculoskeletal system's disorders such as myopathies [15]. Its main aim is to test capabilities of control over such devices based on harder-detectable EMG signals. However, a prototype of a robot mounted at the region of an operator's shoulder girdle may be applied also for the physical works, e.g. in warehouses.

According to the design constraints, an exoskeleton shall be adjustable for most of the population (5th women percentile - 95th men percentile) and have 7 DOFs, including 5 passive DOFs and 2 active DOFs, enabling a free motion of a limb within its whole anatomic range. Complying with Polish legislation law, its load should also not exceed the maximum load of 40 N, permissible for a female worker [3]; however, construction of its end-effector should enable carrying up to 380 N with arm muscles' force. Moreover, its weight and maximum load should not result in a bigger load on a user's shoulder girdle than lifting 8 kg with the straight limb [3].

The construction presented in figure 1 consists of ten bodies, marked with B letters, twelve slide sleeves, marked with S letters and two servo-motors. It is designed as closed loops and to work parallelly to the user's extremity, what minimise torsion and bending stress. An elbow of an operator is supported at the S6/7 while their hand grabs a handle of the S11/12. The exoskeleton is attached to the shoulder girdle by neoprene belts assembled to B1 and it carries the load at TCP.

3. Antropomethric Model

Mechanics of the exoskeleton is design so to enable its usage by most of the population within a whole range of motion in extremities' joints. Therefore it is treated as a parallel mechanism to the multibody model of human limb consisting of three segments - an

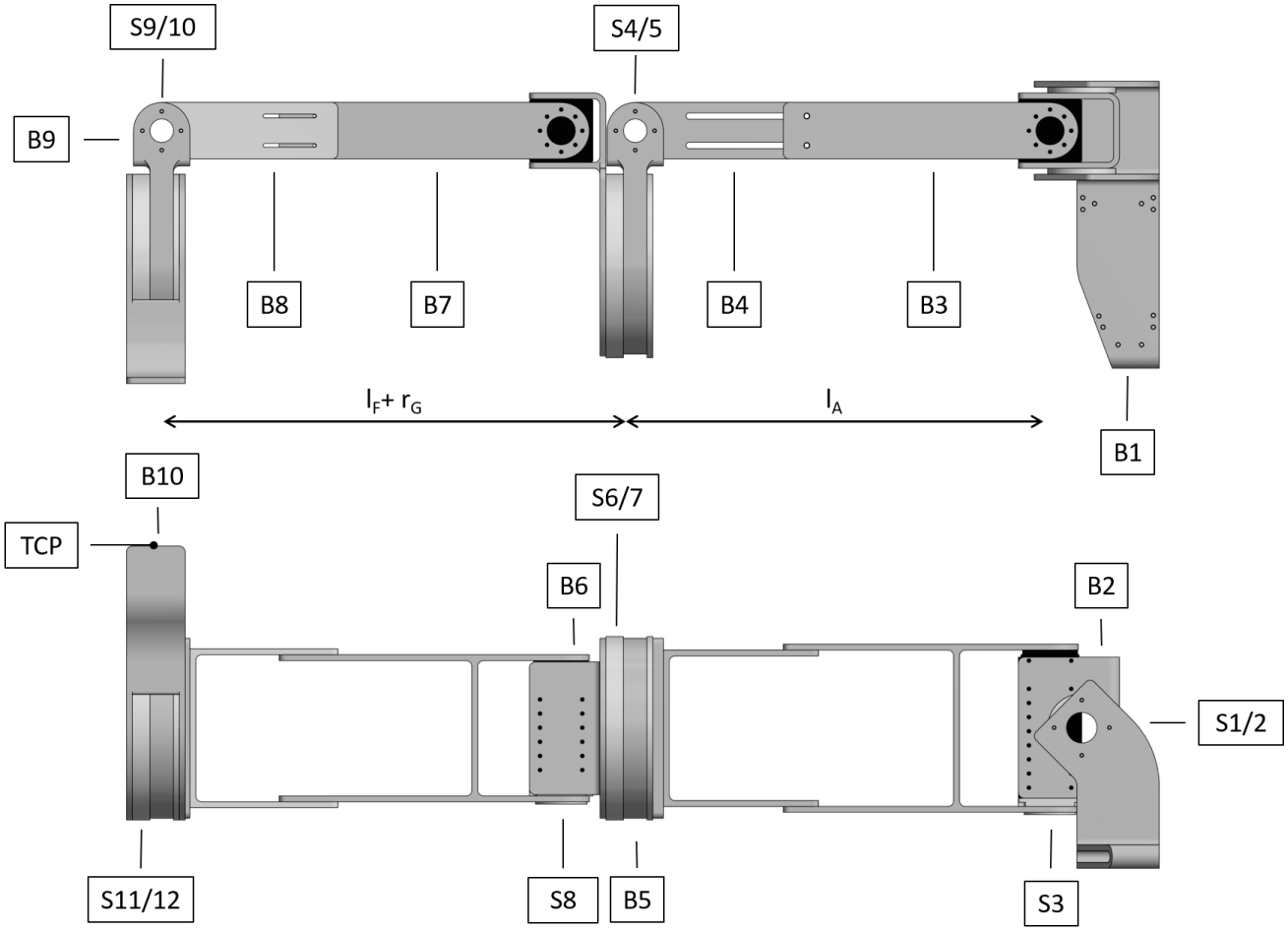

Fig. 1. Schematic design of an exoskeleton

arm, a forearm and a hand (see figure 2). These are connected with shoulder by a 3 DOF joint, and then with each other by 2 DOF joints.

The values of mechanical properties for different segments are estimated for chosen percentiles of the Polish population and afterwards used for dynamics simulations (see table 1, 2) [7] [10]. Considered ranges of anatomical motion of joints are compliant to the *ISOM* standards [12].

Moreover, a pattern of lifting with two human extremities was kinematically modelled as well [14]. As a wrist joint was intended to stay rigid, all the parameters were defined for shoulder and elbow joints and used afterwards for inverse kinematics of a device assembled to the limb (see table 3).

4. Design Cycle

An exoskeleton has been designed within iteration cycles preceded with anthropometric modelling and declaring project constraints. An outcome of the whole process after meeting initial requirements was a complex design of mechanics and printing out chosen parts of the prototype.

4.1. Dynamics Analysis

Motion of an exoskeleton is described with an equation 1 where ${\boldsymbol{r_G}}^{(0)}$ is position of a handle in a frame of reference of a shoulder girdle, $\boldsymbol{R}$ are rotration matrices coresponding to the DOFs of either shoulder φ_S or elbow φ_E joints and the other parameters are the distances between points of intersection of joints' rotation axes (see figure 1).

$$\begin{aligned}{\boldsymbol{r_G}}^{(0)} = \boldsymbol{R_x}(\varphi_{S_x})\boldsymbol{R_y}(\varphi_{S_y})\boldsymbol{R_z^{\uparrow}}(\varphi_{S_z})\Big([l_A,0,0]^T + \\ +\boldsymbol{R_x}(\varphi_{E_x})\boldsymbol{R_z^{\uparrow}}(\varphi_{E_z})\,[l_F+r_G,0,0]^T\Big)\end{aligned} \tag{1}$$

Diverse kinematics and dynamics of a system is computed with respect to inertia of all bodies and gravitational forces. The motion of an end efector is given with trapesium profile of velocity. Selected extremity's joints are activated with asynchronic motion within their anatomic range, while the rotation movement of TCP around its vertical axis is locked. Moreover, TCP is constantly loaded with a force of 40 N.

These simulations affected in a choice of the optimal kinematic scheme from considered (diversified in terms of the type of the first drive and construction of bodies B3 and B4). It required the lowest values of force/torque from the motors and has not limited the motion of a user's elbow by the mechanism (see figure 3).

4.2. Materials and Production Technology Selection

As an exoskeleton supposed to be easily modified and cheap to build in the prototyping process, its ini-

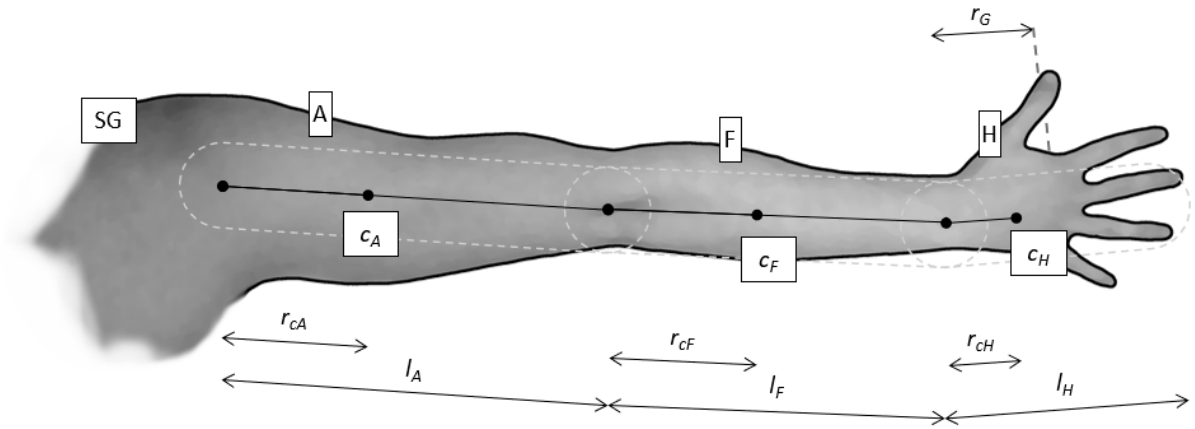

Fig. 2. Scheme of used model of a human upper extremity with involved parameters

Tab. 1. Lengths [mm] and masses [kg] of segments of a human upper extremity

Percentile	l_A	l_F	l_H	r_G	r_{c_A}	r_{c_F}	d_A	d_F	r_{c_H}	m_A	m_F	m_H
W5	286	189	179	115	125.84	81.27	76.39	66.23	67.16	1.50	0.78	0.50
M50	349	235	196	117	153.56	101.05	95.49	72.52	87.22	2.35	1.21	0.78
M95	383	273	210	125	168.52	117.39	109.5	77.70	98.04	2.97	1.54	0.99

Tab. 2. Main moments of inertia of segments of a human upper extremity $[kg \cdot m^2]$

Percentile	I_{xx_A}	I_{xx_F}	I_{xx_H}	I_{yy_A}	I_{yy_F}	I_{yy_H}	I_{zz_A}	I_{zz_F}	I_{zz_H}
W5	0.395	0.317	0.067	0.420	0.326	0.054	0.109	0.061	0.024
M50	1.254	0.822	0.125	1.340	0.842	0.103	0.269	0.128	0.125
M95	1.861	1.144	0.159	2.011	1.175	0.130	0.413	0.186	0.159

Tab. 3. Maximum kinematic parameters of shoulder and elbow joints during lifting with two limbs involved

Joint	**Type of motion**	$\varphi[^o]$	$\omega[rad/s]$	$\varepsilon[rad/s^2]$
Shoulder joint	Flexion	135	3,0	23,0
	Extension	25	2,3	22,4
	Adduction	60	1,7	12,5
	Abduction	5	3,0	23,0
	External rotation	20	2,0	17,8
	Internal rotation	-75	2,4	18,3
Elbow joint	Flexion	135	2,6	19,5
	Extension	40	2,0	19,4
	External rotation	30	1,0	8,2
	Internal rotation	-25	1,2	8,2

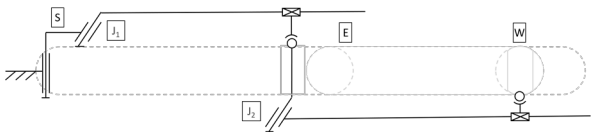

Fig. 3. Chosen kinematic scheme of an exoskeleton

tial version was designed from thermoplastic material. Thus, it enabled 3-D printing with FFF technology by using a simple *Prusa MK3s* printer.

Main bodies (B) were to be made of a filament with high-durability, *Compositum ABS ST*^{TM} [1], while all the sleeves (S) were to be made of a sliding filament, *iglidur®I180-PF* [2]. However, outcomes of FEM analysis caused a change of the material for bodies into CFRP composite *T300/914* [9] and division of sleeves' structure into the inner supporting sleeve from *T300/914* and outer sliding sleeve from *iglidur®I180-PF*.

4.3. FEM Analysis

FEM analysis has been run in *Autodesk Inventor 2018* environment separately for every body of an exoskeleton (B1-B10). Each of them was rigidly supported at the point of connection with a previous body and loaded with a maximum reaction force computed in the forward dynamics at the point of connection with the next body. Apart from reaction forces including inertia of parts, a gravitational acceleration was implemented into the study.

To minimise the mass needed for strength, stiffness and durability constraints, an optimal direction of beams in printouts was chosen (see table 4, where orientation is described by the two letters standing for head-bed surface according to CAD project, where the first letter describes an axis from the project aligned with printout's beams). They were aligned with a vector of maximum reaction force occurring in a body during its simulated motion.

Afterwards, every part was divided into tetrahedral elements with 8 nodes each (see table 4) and as-

Tab. 4. Details of used FEM mesh grids and parts' orientations

Part	Nodes	Elements	Final material	Material of a prototype	Orientation
B1	10,238	5,144	T300/914	Compositum ABS ST	xz
B2	21,589	11,202	T300/914	Compositum ABS ST	xz
B3	3,884	1,796	T300/914	Compositum ABS ST	zy
B4	3,127	1,358	T300/914	Compositum ABS ST	zx
B5	2,581	1,131	T300/914	Compositum ABS ST	yz
B6	9,452	4,564	T300/914	Compositum ABS ST	yz
B7	4,621	2,142	T300/914	Compositum ABS ST	zy
B8	4,137	1,898	T300/914	Compositum ABS ST	zy
B9	2,581	1,131	T300/914	Compositum ABS ST	yz
B10	3,418	1,562	T300/914	Compositum ABS ST	xy

signed to orthotropic material *Compositum ABS ST™* with strength parameters scaled according to experimental values for typical ABS [4], based on its nominal mechanical parameters (see table 5).

The analysis was carried to check the design compliance with the strength and stiffness conditions, as significant deviations occurring in the parts are compensated by their parallel connection to the human extremity.

Tab. 5. Mechanical parameters of an orthotropic model of *Compositum ABS ST™* material

Direction	xx	yy	zz	Nominal
R_m [Mpa]	35.23	38.56	23.74	51.2
F_u [kN]	1.41	1.54	0.95	2.05
E [Mpa]	2716.44	2730.67	2375.11	3431.82
ν	0.46	0.57	0.44	0.48
G [Mpa]	1023	977	906	1280

4.4. Topology Optimisation

To make a design as light as it is possible, the topology optimisation module of *Autodesk Inventor 2018* has been used as well. Previously defined meshes and materials (see table 4) were used. FEM analysis was in prior to any modification and then certain elements were removed from the mesh to keep elastic potential energy minimal according to the formula 2, where $\boldsymbol{K_e}$ is a stiffness matrix of an element e, E_e is a field of the stiffness of an element e and $\boldsymbol{u}$ is a vector of displacements [13].

$$min \left(\sum_{e=1}^{N} \boldsymbol{K_e} \left(E_e \right) \boldsymbol{u} \right)^T \boldsymbol{u} \quad \forall E_e \in E_a \tag{2}$$

Additionally, constraints on some areas were added. Elements from the close neighbourhood of wholes and bearings were not removable. Moreover, the symmetry planes were defined as well. Also, every part had to stay in one piece at the end of optimisation.

The whole process was repeated until the final mass could not be reduced without splitting the part into halves or until results of FEM analysis of modified body were insufficient. Based on the refragmented design, a new one was created by removing material from selected areas. The results of maximum mass reductions are presented in a table 6. Topological optimisation decreased mass of an initially-designed exoskeleton by 15%.

Tab. 6. Results of a strength analysis of the exoskeleton's parts before and after topology optimisation

Part	Mass red.	m [g]	σ_{red} [Mpa]	ε[%]	d [mm]
B1	0%	367	4.911	0.004	0.044
B2	0%	172	1.949	0.001	0.002
	5%	163	2.178	0.001	0.002
B3	0%	205	12.782	0.001	0.0164
	16%	173	14.185	0.001	0.016
B4	0%	137	43.189	0.03	0.001
B5	0%	248	0.291	0.001	0.001
	26%	184	28.459	0.02	0.016
B6	0%	223	51.143	0.038	0.088
	14%	192	5.56	0.04	0.065
B7	0%	208	24.868	0.019	0.39
	15%	177	27.046	0.021	0.537
B8	0%	123	16.927	0.012	0.024
	18%	101	16.253	0.011	0.034
B9	0%	248	0.291	0.001	0.001
	26%	184	0.852	0.001	0.001
B10	0%	267	27.846	0.02	0.101
	27%	194	35.154	0.024	0.127

4.5. Rapid Prototyping

To validate the design rapidly, both sliding sleeves and parts from ABS were printed with *Prusa MK3s* printer. Elements made of *Compositum ABS ST™* kept high accuracy and the tolerance of their dimensions stayed within a range of ± 1 mm; even though, the printer was not covered with any enclosure. To achieve

smaller roughness, the designs could be enhanced by additional outer trails and then ground. However, this was not necessary in this case. Regions were the screws supposed to be were printed with 100% fill to enable drilling and threading. Sleeves made of *iglidur®I180-PF* required additional post-machining. Their dimensional tolerance stayed within a range of ± 2 mm; thus, the design was enhanced by additional outer trails and then ground significantly. Thanks to this, relatively big roughness was decreased to the value permissible for the designed bearings.

5. Human Compatibility

5.1. Control System

The exoskeleton was designed to broaden capabilities of direct control over such constructions with EMG signals. Thus, the electrodes were designated to be placed in the regions corresponding to four major muscles of a shoulder girdle (SP - pectoralis major, AD - deltoideus, TM - teres major and LD - latissimus dorsi) and two muscles of an arm (BB - biceps brachii and TB - triceps brachii) [6]. Then the simple schematic model of a control system was performed. However, it had significant biases caused by its dependence on measured and estimated anatomical parameters of a user, such as masses and lengths of limb's segments. Therefore, it was ineffective for universal application by various operators.

5.2. Equipment Placement

Apart from the designed construction assembled to the region of shoulder girdle and blade by neoprene belts, the device consisted of a battery and a control system board. As these both need to be carried by a user, they affect the load on a musculoskeletal system.

To minimise the forces affecting spine extensor a simulation based on Stotte's model was run [8]. It assumed a point force load from the battery weight equal to 15 N and a point force load from the weight of a control panel hardware equal to 5 N. Also to decrease a force affecting oblique muscles, minimisation of a moment of force in a coronal plane was performed. Results of both calculations determined that the battery and a control system board should be attached right above pelvis of a user on the other side of the torso than the exoskeleton (symmetrically regarding sagittal plane). Moreover, the battery should be placed in their back, while the board should stay in their front.

6. Conclusion

The designed exoskeleton is fully applicable for pre-defined tests on the efficacy of a direct control based on EMG signals. Moreover, it may be also applied for patients with musculoskeletal disorders to support their lifting capabilities.

A presented approach towards mechanical design involving orthotropic modelling of parts 3D printed within FFF technology from different materials, and their further topologic optimisation and FEM strength analysis, enabled significant decrement of a mass of construction. If the device would be commercialised, its sliding sleeves should be topologically optimised as well.

As an initial design, it may also be significantly improved. Further stages of the project might include complex dynamic user's musculoskeletal system analysis and deep UX research. Also, the bodies could be printed from a cheaper material, not necessarily involving FFF technology, and the chosen servo-drives could be replaced by the ones generating higher torques and rotational velocities.

Apart from its initial aim, the exoskeleton could be used for tests on EEG capabilities or support lifting in warehouses after strengthening of bodies' constructions.

AUTHOR

Piotr Falkowski – Warsaw University of Technology, ŁUKASIEWICZ Research Network – Industrial Research Institute for Automation and Measurements PIAP, Al. Jerozolimskie 202, 02-486 Warsaw, Poland, e-mail: piotr.falkowski@piap.lukasiewicz.gov.pl, www: https://piap.pl/.

REFERENCES

[1] "Compositum ABS ST™". http://www.corotechnology.com/english/compositum-filament-series/compositum-abs-st/. Accessed on: 2021-12-21.

[2] "iglidur® I180-PF, filament do drukarki 3D". https://igus.widen.net/content/5xyi4cs8uh/original/3DP_DS_iglidur_I180-PF_Product_Data_Sheet_EN_1.pdf. Accessed on: 2021-12-21.

[3] "Rozporządzenie Ministra Rodziny, Pracy i Polityki Społecznej z dnia 25 kwietnia 2017 r. zmieniające rozporządzenie w sprawie bezpieczeństwa i higieny pracy przy ręcznych pracach transportowych". http://isap.sejm.gov.pl/isap.nsf/DocDetails.xsp?id=WDU20170000854. Accessed on: 2021-12-21.

[4] M. Cader, *Szacowanie wytrzymałości prototypów wytwarzanych przyrostowo metodą FDM*, Oficyna Wydawnicza PIAP: Warszawa, 2016, (in Polish).

[5] R. Dindorf, "Rozwój i zastosowanie manipulatorów i robotów rehabilitacyjnych", *Pomiary Automatyka Robotyka*, vol. 7, no. 11, 2004, 5–9, (in Polish).

[6] K. Fukuda, H. Tottori, K. Kameoka, T. Ono, and K. Yoshida, "A method for estimating axle weights of in-motion vehicles and its evaluation". In: *Proc. of the 41st SICE Annual Conference. SICE 2002.*, vol. 2, Osaka, Japan, 2002, 1014–1018, 10.1109/SICE.2002.1195309.

[7] A. Gedliczka and P. Pochopień, *Atlas miar człowieka: dane do projektowania i oceny ergonomicznej: antropometria, biomechanika, przestrzeń pracy, wymiary bezpieczeństwa*, Centralny Instytut Ochrony Pracy: Warszawa, 2001, (in Polish).

[8] M. Gzik, *Biomechanika kręgosłupa człowieka*, Wydawnictwo Politechniki Śląskiej: Gliwice, 2008, (in Polish).

[9] A. Lowe, "Transverse compressive testing of T300/914", *J. Mater. Sci.*, vol. 31, no. 4, 1996, 1005–1011, 10.1007/BF00352901.

[10] J. T. McConville, C. E. Clauser, T. D. Churchill, J. Cuzzi, and I. Kaleps. "Anthropometric Relationships of Body and Body Segment Moments of Inertia". Technical Report AFAMRL-TR-80-119, Anthropology Research Project, Inc., Yellow Springs, Ohio, USA, 1980.

[11] E. Mikołajewska and D. Mikołajewski, "Wykorzystanie robotów rehabilitacyjnych do usprawniania", *Niepełnosprawność - zagadnienia, problemy, rozwiązania*, vol. 3, no. 4, 2013, 21–44, (in Polish).

[12] M. Pajor and P. Herbin, "Egzoszkielet kończyny górnej - model z wykorzystaniem rzeczywistych parametrów ruchu", *Modelowanie Inżynierskie*, vol. 26, no. 57, 2015, 40–46, (in Polish).

[13] P. Poszwa and M. Szostak, "Topological optimization of the design of products manufactured by injection molding of plastics", *Mechanik*, vol. 90, no. 11, 2017, 948–950, 10.17814/mechanik.2017.11.151.

[14] J. Rosen, J. Perry, N. Manning, S. Burns, and B. Hannaford, "The human arm kinematics and dynamics during daily activities - toward a 7 DOF upper limb powered exoskeleton". In: *Proc. 12th International Conference on Advanced Robotics, ICAR 2005*, Seatle, WA, USA, 2005, 532–539, 10.1109/ICAR.2005.1507460.

[15] M. A. Samuels, *Manual of Neurologic Therapeutics*, Lippincott Williams & Wilkins, 2004.